

Quaternion-based Adaptive Backstepping Fast Terminal Sliding Mode Control for Quadrotor UAVs with Finite Time Convergence

Arezo Shevidi and Hashim A. Hashim

Abstract—This paper proposes a novel quaternion-based approach for tracking the translation (position and linear velocity) and rotation (attitude and angular velocity) trajectories of underactuated Unmanned Aerial Vehicles (UAVs). Quadrotor UAVs are challenging regarding accuracy, singularity, and uncertainties issues. Controllers designed based on unit-quaternion are singularity-free for attitude representation compared to other methods (e.g., Euler angles), which fail to represent the vehicle's attitude at multiple orientations. Quaternion-based Adaptive Backstepping Control (ABC) and Adaptive Fast Terminal Sliding Mode Control (AFTSMC) are proposed to address a set of challenging problems. A quaternion-based ABC, a superior recursive approach, is proposed to generate the necessary thrust handling unknown uncertainties and UAV translation trajectory tracking. Next, a quaternion-based AFTSMC is developed to overcome parametric uncertainties, avoid singularity, and ensure fast convergence in a finite time. Moreover, the proposed AFTSMC is able to significantly minimize control signal chattering, which is the main reason for actuator failure and provide smooth and accurate rotational control input. To ensure the robustness of the proposed approach, the designed control algorithms have been validated considering unknown time-variant parametric uncertainties and significant initialization errors. The proposed techniques has been compared to state-of-the-art control technique.

Index Terms—Adaptive Backstepping Control (ABC), Adaptive Fast Terminal Sliding Mode Control (AFTSMC), Unit-quaternion, Unmanned Aerial Vehicles, Singularity Free, Pose Control

I. INTRODUCTION

A. Motivation

IN recent years, Unmanned Aerial Vehicles (UAVs) application, commonly known as drones, has witnessed a surge in research interest. These cutting-edge advanced devices have captured significant attention due to remarkable adaptability, low energy consumption, and small size [1]–[6]. The convergence of breakthroughs in electric power storage, wireless communication [7], agriculture, space exploration, and firefighting has been pivotal in propelling the development of innovative drone models [3], [4], [7]–[9]. Among various kinds of drones, quadrotors represent a nascent and highly versatile category of UAVs, showing interesting advancements in diverse applications. Quadrotors are used in various fields,

from logistics, delivery services, and environmental conservation efforts to search and rescue operations, building inspection and reconnaissance, maintenance tasks, precision agriculture, videography and photography, mining operations, as well as hazardous activities [3], [4], [9]–[11]. Moreover, quadrotors provide remarkable adaptability for indoor and outdoor flights, enabling deployment in underwater environments, over water surfaces, terrestrial landscapes, airspace, and even outer space, further enhancing its operational flexibility [10]. Quadrotors hold inherent positive features that distinguish them from conventional helicopters, making them in high demand for various practical applications [11], [12]. The features stem from the lightweight structure and streamlined mechanical system, enabling them to guarantee stable hover flight, which is a crucial prerequisite in real applications. Such attributes not only optimize flight performance but also improve operational safety [11]–[13]. Moreover, quadrotors can maneuver precisely in close quarters, enabling them to perform vertical take-offs and navigate through cluttered and confined spaces [14]. As a result, quadrotors serve as invaluable aids in various daily tasks and prove particularly indispensable in tackling complex and hazardous missions [14]. However, despite their many advantages, quadrotors encounter significant challenges primarily linked to the rotation of their propellers and the flapping of their blades [15]. Furthermore, the strong interdependence between their position and attitude amplifies the complexity of their control systems, characterized by underactuation and susceptibility to disturbances arising from aerodynamic effects, including sensitivity to wind gusts, thereby compromising stability [14], [16].

B. Related Work and Challenges

The control of UAVs presents notable limitations and challenges that arise from model representations and control design. Several control strategies and approaches have been investigated to tackle control system limitations, including singularity, stability, and chattering [11], [17]–[21]. For instance, [18] has proposed a conventional PID-based controller for attitude control. Also, in [22], state-dependent Linear Quadratic Regulator (LQR) control is suggested. In [21], nonlinear model predictive control (NMPC) is developed to navigate and avoid obstacles for UAVs. In [11], [12], nonlinear cascaded vision-based controllers that relies on Lyapunov stability have been developed. In [23], multi-trajectory MPC is explored for UAV navigation while the environment is

This work was supported in part by National Sciences and Engineering Research Council of Canada (NSERC), under the grants RGPIN-2022-04937 and DGEER-2022-00103.

A. Shevidi and H. A. Hashim are with the Department of Mechanical and Aerospace Engineering, Carleton University, Ottawa, Ontario, K1S-5B6, Canada, (e-mail: hhashim@carleton.ca).

unknown. Authors investigate robust MPC to handle the mismatch uncertainty of the model or external disturbance. They designed the robust MPC by defining optimization problems with constraints in [23]–[25]. Although the MPC approach is an advanced control technique based on prediction and optimization, its implementation is not cost-effective in practical application. Moreover, the computational burden is the major disadvantage of NMPC. In addition, the above-listed controllers are not characterized with finite-time convergence. Among the mentioned control strategies, Sliding Mode Control (SMC) has gained significant attention regarding simplicity, accuracy, and handling uncertainties. In [26], [27], SMC is utilized to control UAV systems, robotics, navigation, and aircraft guidance. For example, in [26], the work developed a fractional order SMC for a quadrotor with varying load. The main point of the controller is to provide missile guidance in the presence of uncertainty [26]. In [27], the authors use adaptive SMC to control robot manipulators.

SMC, despite its streamlined implementation and robustness, holds critical drawbacks such as (1) Chattering (2) Finite-time issues (3) Performance during reaching phase [28]–[31]. Chattering and oscillation caused by switching control action can be a critical issue in SMC. In practical flight applications, chattering can be considered one of the negative consequences of SMC because of its critical impact on the stability and robustness of an actuator system [28], [32]. Regarding the finite time issue, SMC may not guarantee convergence to desired states in the finite time since the sliding surface is designed in a linear form. In other words, while the system gradually reaches the sliding surface, the convergence time may even be unbounded depending on the specific initial conditions. Additionally, according to [29], [30], during the reaching phase, SMC may not be robust, and the system may be susceptible to instability in the presence of external disturbances. Moreover, convergence can be more complicated if the states are not close to equilibrium points [30]. To improve the performance of controllers, advanced sliding mode techniques have been developed to remove chattering, ensure finite time convergence, and enhance performance in [20], [33]–[40]. In [33], a fast terminal sliding mode control is designed to reduce the effect of chattering while the quadrotor is under uncertainties. The work in [34] implemented super twisting SMC to improve the performance of the fully-actuated UAVs in speed tracking with fast convergence. In [36], more efforts have been made to enhance stability, while uncertainty and external disturbances exist in UAVs. The fractional order non-singular TSMC with adaptation laws is used to overcome external disturbances and uncertainties for advanced layout carrier-based UAV [36]. [37] has explored dynamic SMC with adaptive control which is tolerable in the presence of faults and fixed-time disturbance. The work in [38] investigated the mixture of the nonlinear observer with SMC to overcome UAV system faults. The work in [39], [40] combines neural networks with FTSMC to design fault-tolerant control for UAVs.

Tackling underactuation represents the first challenge. The majority of the UAVs are considered to be underactuated systems, which is a fundamental challenge for achieving robust

and reliable missions [12]. From realistic and practical points of view, having control over all states is often impossible. Due to such a fundamental deficiency, stabilizing and achieving desired tasks become a complex challenge. Unfortunately, most of the above-listed control systems have been designed for fully-actuated UAVs, which is a fundamental challenge (e.g., an adaptive and super-twisting sliding mode controller [20]). However, such an assumption is not realistic nor practical for the majority of UAVs. In this regard, backstepping is an effective approach to address under-actuation issues. The main idea of backstepping is to generate an intermediary control input (virtual control), done in a cascaded way to tackle the limitation of underactuated control system [41]. The second challenge is avoiding singularity in each control design and attitude representation to ensure UAV stabilization. Although the above-listed techniques have attempted to avoid singularity and chattering, the designed controllers are based on Euler angles, which can lead to a significant issue in tracking and UAV stability [11]. Unit-quaternion can be an alternative method to represent attitude without singularity issues. In particular, Euler angles hold significant shortcomings, such as kinematic singularities and local representation [42]. Such an issue causes the controller to fail, resulting in undesired performance.

C. Contributions

In this paper, we consider cascaded control design and adopt quaternion-based ABC to handle the UAV underactuated issues leveraging an auxiliary control input (virtual control). The auxiliary control of ABC generates the required thrust and the desired UAV orientation for attitude control. In addition, with the novel quaternion-based controllers, we resolve the persistent singularity shortcomings of other common methods in literature (e.g. Euler-based controller). Afterwards, we mitigate chattering issues of the control signal, the fundamental reason for actuator damage, by modifying the sliding surface. The “fast” and adaptive aspects of the proposed quaternion-based AFTSMC are crucial in reducing chattering problems. Also, The finite-time convergences with smooth control signals are guaranteed by the established quaternion-based AFTSMC compared to conventional Euler-based SMC. In order to enhance the robustness of the proposed controllers, the adaptive features of proposed controllers are developed to adjust control parameters while unknown time-varying parametric uncertainties and significant initialization errors exist. The main contributions are as follows:

- (1) A novel quaternion-based ABC is proposed to control the UAV translation dynamics by addressing the underactuated issues via an auxiliary control input (virtual control).
- (2) A quaternion-based AFTSMC is proposed for the UAV rotational dynamics to mitigate the chattering (the main reason for actuator failure) by fast and non-singular features of the sliding surface with adaptation control parameters.
- (3) The proposed attitude quaternion-based controller guarantees states converge to desired values in finite time with smooth control signal.

TABLE I: Nomenclature

$\{\mathcal{B}\}$:	Body-frame (moving-frame)
$\{\mathcal{I}\}$:	Inertial-frame (fixed-frame)
I_{xx}, I_{yy}, I_{zz}	:	UAV inertia
J	:	Inertia matrix
m	:	Mass of the UAV
g	:	Gravitational acceleration
$X = [x_p, y_p, z_p]^\top$:	True position of the UAV
$X_d = [x_d, y_d, z_d]^\top$:	Desired position of the UAV
$V = [v_1, v_2, v_3]^\top$:	Linear velocity of the UAV
R	:	Rotational matrix (True UAV orientation)
$\Omega_B = [p_v, q_v, r_v]^\top$:	UAV angular velocity in body-frame
Ω_d	:	Desired angular velocity
Ω_e	:	Angular velocity error
R_e	:	Rotational matrix error
Q	:	Unit quaternion (True UAV orientation)
Q_d	:	Desired Unit quaternion
$Q_e = [e_0, e^\top]$:	Quaternion error
$\mathcal{T} = [\mathcal{T}_1, \mathcal{T}_2, \mathcal{T}_3]$:	Rotational torque input
F_{th}	:	Total thrust
e_{xp}, e_{yp}, e_{zp}	:	Position error
e_{v1}, e_{v2}, e_{v3}	:	Linear velocity error
$\hat{n}_{x2}, \hat{n}_{y2}, \hat{n}_{z2}$:	Adaptive estimate (position control parameters)
$\hat{k}_1, \hat{k}_2, \hat{k}_3$:	Adaptive estimate (attitude control parameters)
s	:	FTSMC surface
U_x, U_y, U_z	:	Virtual control

- (4) The innovative quaternion-based controllers addresses the persisting challenge of Euler angles-based solutions, namely kinematic singularity and failure of model representation at certain configuration.

The novel control systems utilize adaptation mechanisms and guarantee asymptotic stability using the Barbalet Lemma and Lyapunov theorem. The simplicity and straightforward design approach is not only safer but also more autonomous in flight missions compared to other methods in the literature.

A comparison to state-of-the-art controllers for UAVs has been included.

D. Structure

The remaining of the paper is summarized as follows: In Section II, the preliminaries and math notation are provided. Section III presents the UAV model in quaternion representation. Section IV introduces problem formulation and proposes quaternion-based controllers. Section V introduces the implementation steps. Section VI depicts the simulation results confirming the effectiveness of the proposed controller. Finally, section VII summarizes the paper.

Some of the commonly used notation is provided in Table I.

II. PRELIMINARIES

A. Math Notation

In this paper, \mathbb{R} describes the set of real numbers. $\mathbb{R}^{c \times d}$ represents the set of real-numbers with dimensional space c -by- d . $\mathbf{I}_c \in \mathbb{R}^{c \times c}$ and $\mathbf{0}_c \in \mathbb{R}^{c \times c}$ represent identity and zero matrices, respectively. $\|y\| = \sqrt{y^\top y}$ refers to an Euclidean norm of the column vector $y \in \mathbb{R}^n$. Let $[v]_\times$ denote a skew-symmetric matrix such that

$$[v]_\times = \begin{bmatrix} 0 & -v_3 & v_2 \\ v_3 & 0 & -v_1 \\ -v_2 & v_1 & 0 \end{bmatrix}, \quad v = \begin{bmatrix} v_1 \\ v_2 \\ v_3 \end{bmatrix}$$

For $M \in \mathbb{R}^{3 \times 3}$ and $w, v \in \mathbb{R}^3$, the following characteristics hold true [11], [12]:

$$\begin{aligned} -[v]_\times v &= \mathbf{0}_{3 \times 1} \\ [w]_\times^\top &= -[w]_\times \\ [w]_\times v &= -v[w]_\times \\ [Mv]_\times &= M[v]_\times M^\top \end{aligned} \quad (1)$$

In this work, we consider a UAV travelling in 3D space where the vehicle's moving-frame (body-frame) is denoted by $\{\mathcal{B}\} = \{x_B, y_B, z_B\}$ while the inertial-frame is described by $\{\mathcal{I}\} = \{x_p, y_p, z_p\}$.

B. Unit-quaternion

Unit-quaternion is a useful tool for singularity-free attitude (orientation) representation in 3D space. Q is a unit-quaternion vector such that $Q = [q_0, q_1, q_2, q_3]^\top = [q_0, \mathbf{q}^\top]^\top \in \mathbb{R}^4$ and $\|Q\| = 1$ [12], [42] where $q_0 \in \mathbb{R}$ and $\mathbf{q} = [q_1, q_2, q_3]^\top \in \mathbb{R}^3$. The unit-quaternion four elements are given as follows [42]:

$$Q = q_0 + iq_1 + jq_2 + kq_3$$

where $i, j,$ and k refers to the standard basis-vectors. Q^{-1} denoted inversion of Q and is given by [11]:

$$Q^{-1} = Q^* = [q_0, -q_1, -q_2, -q_3]^\top = [q_0, -\mathbf{q}^\top]^\top \in \mathbb{R}^4$$

Consider \otimes to be quaternion multiplication and let $Q = [q_0, \mathbf{q}^\top]^\top$ and $Q_d = [q_{0d}, \mathbf{q}_d^\top] = [q_{0d}, q_{1d}, q_{2d}, q_{3d}]^\top$ be two quaternion vectors describing true and desired UAV attitude, respectively, where $q_0, q_{0d} \in \mathbb{R}$ and $\mathbf{q}, \mathbf{q}_d \in \mathbb{R}^3$. The quaternion multiplication of Q and Q_d is given by:

$$Q \otimes Q_d = \begin{bmatrix} q_0 q_{0d} + \mathbf{q}^\top \mathbf{q}_d \\ q_{0d} \mathbf{q} - q_0 \mathbf{q}_d + [\mathbf{q}]_\times \mathbf{q}_d \end{bmatrix} = \begin{bmatrix} e_0 \\ e \end{bmatrix}$$

Quaternion multiplication is associative but not commutative. The UAV attitude representation in form of a rotational matrix described with respect to the Lie Group of the Special Orthogonal Group $SO(3)$ is described by

$$R = (q_0^2 - \mathbf{q}^\top \mathbf{q}) \mathbf{I}_3 + 2\mathbf{q}\mathbf{q}^\top + 2q_0[\mathbf{q}]_\times \in SO(3) \subset \mathbb{R}^{3 \times 3}$$

Which is equivalent

$$R = \begin{bmatrix} 1 - 2(q_2^2 + q_3^2) & 2(q_1 q_2 - q_0 q_3) & 2(q_1 q_3 + q_0 q_2) \\ 2(q_2 q_1 + q_0 q_3) & 1 - 2(q_1^2 + q_3^2) & 2(q_2 q_3 - q_0 q_1) \\ 2(q_3 q_1 - q_0 q_2) & 2(q_3 q_2 + q_0 q_1) & 1 - 2(q_1^2 + q_2^2) \end{bmatrix} \in SO(3) \quad (2)$$

where $\det(R) = +1$ and $RR^\top = \mathbf{I}_3$ with $\det(\cdot)$ being determinant of a matrix and $R \in \{\mathcal{B}\}$.

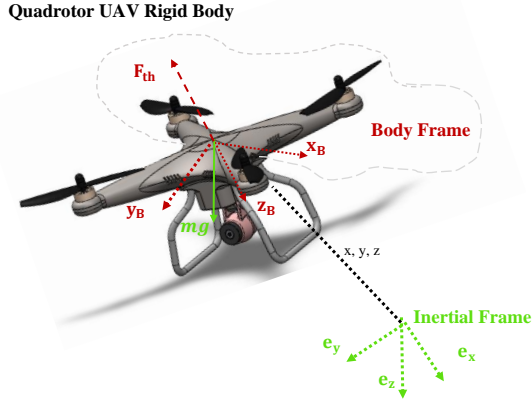


Fig. 1: Quadrotor UAV configuration

III. UAV DYNAMICAL MODEL AND QUATERNION REPRESENTATION

The structure of the quadrotor consists of four rotors where the blades rotate via rotors in such a direction to produce thrust. In this regard, the flight motion of a UAV consists of two parts, namely, translation and rotation [11], [33]. The structure of a quadrotor UAV is presented in Figure 1. Note that the under-actuation nature of UAV requires a cascaded design of the controller, translational controller (outer part) and rotational controller (inner part). In the translation part, the UAV controller is tasked with thrust generation to follow predefined desired position trajectories x_d , y_d , and z_d . In the rotation part, the UAV controller is tasked with generating rotational torques to follow predefined attitude trajectories $Q_d = [q_{0d}, q_{1d}, q_{2d}, q_{3d}]$ produced by the translational controller (outer part).

A. UAV Translation and Rotational Dynamics

The UAV translation dynamics are given as follows [11], [12]

$$\text{Translation : } \begin{bmatrix} \dot{X} \\ \dot{V} \end{bmatrix} = \begin{bmatrix} V \\ \begin{bmatrix} 0 \\ 0 \\ g \end{bmatrix} + m^{-1}RU \end{bmatrix} \quad (3)$$

where m and g are mass and gravity acceleration, respectively, $U = [0, 0, -F_{th}]^T \in \mathbb{R}^3$ is the total input control for translation state space equation of UAV and F_{th} is the total thrust. $X = [x_p, y_p, z_p]^T \in \mathbb{R}^3$ denotes UAV's true position, $V = [v_1, v_2, v_3]^T \in \mathbb{R}^3$ denotes UAV's true velocity, and $R \in SO(3) \subset \mathbb{R}^{3 \times 3}$ denotes UAV true attitude described in (2) where $X, V \in \{\mathcal{I}\}$ and $R \in \{\mathcal{B}\}$. The UAV rotation dynamics are defined by [11], [12], [43]:

$$\text{Rotation } \begin{cases} \dot{R} &= -[\Omega_B]_{\times} R \\ J\dot{\Omega}_B &= [J\Omega_B]_{\times} \Omega_B + \mathcal{T}, \end{cases} \quad (4)$$

where $\Omega_B = [p_v, q_v, r_v]^T \in \mathbb{R}^3$, $R \in SO(3)$, $\mathcal{T} = [\mathcal{T}_1, \mathcal{T}_2, \mathcal{T}_3]^T \in \mathbb{R}^3$ are UAV's angular velocity, attitude, and torque input, respectively, with $R, \Omega_B, \mathcal{T} \in \{\mathcal{B}\}$, and

$J \in \mathbb{R}^{3 \times 3}$ refers to the inertia matrix which is symmetric. Based on (4), the equivalent attitude dynamics in quaternion form are given by [11], [12]:

$$\text{Rotation } \begin{cases} \dot{q}_0 &= -\frac{1}{2} \mathbf{q}^T \Omega_B \\ \dot{\mathbf{q}} &= \frac{1}{2} (q_0 \Omega_B + [\mathbf{q}]_{\times} \Omega_B) \\ J\dot{\Omega}_B &= [J\Omega_B]_{\times} \Omega_B + \mathcal{T} \end{cases} \quad (5)$$

with $Q \in \mathbb{S}^3$ being UAV's orientation with respect to unit-quaternion.

Assumption 1. It is assumed that the structure of UAV is symmetric and rigid.

Assumption 2. The desired position $X_d = [x_d, y_d, z_d]^T \in \mathbb{R}^3$ is assumed to be bounded and twice differentiable.

B. Expanded Vehicle Nonlinear Dynamics

By substituting (2) in (3), the expanded state space equations of the UAV translation dynamics can be described by:

$$\begin{cases} \dot{x}_p &= v_1 \\ \dot{v}_1 &= -2m^{-1}F_{th}(q_0q_2 + q_1q_3) \\ \dot{y}_p &= v_2 \\ \dot{v}_2 &= -2m^{-1}F_{th}(q_2q_3 - q_0q_1) \\ \dot{z}_p &= v_3 \\ \dot{v}_3 &= -m^{-1}F_{th}(q_0^2 - q_1^2 - q_2^2 + q_3^2) + g \end{cases} \quad (6)$$

Expanding (5) results in the following rotational dynamics:

$$\begin{cases} \dot{p}_v &= I_{xx}^{-1}((I_{yy} - I_{zz})q_v r_v + \mathcal{T}_1) \\ \dot{q}_v &= I_{yy}^{-1}((I_{zz} - I_{xx})r_v p_v + \mathcal{T}_2) \\ \dot{r}_v &= I_{zz}^{-1}((I_{xx} - I_{yy})p_v q_v + \mathcal{T}_3) \end{cases} \quad (7)$$

Likewise, in the light of (5), the quaternion orientation dynamics are given by:

$$\begin{cases} \dot{q}_0 &= -\frac{1}{2}(q_1 p_v + q_2 q_v + q_3 r_v) \\ \dot{q}_1 &= \frac{1}{2}(q_0 p_v - q_3 q_v + q_2 r_v) \\ \dot{q}_2 &= \frac{1}{2}(q_3 p_v + q_0 q_v - q_1 r_v) \\ \dot{q}_3 &= \frac{1}{2}(-q_2 p_v + q_1 q_v + q_0 r_v) \end{cases} \quad (8)$$

IV. PROBLEM FORMULATION AND CONTROLLER DESIGN

Solving singularity and chattering issues involves making autonomous UAV safer, more efficient, and more integrated into diverse applications. The main goal of this section is to design robust and singular-free controllers for the UAV to follow predefined desired trajectories, namely desired position $X_d = [x_d, y_d, z_d]^T \in \mathbb{R}^3$ and desired attitude $Q_d = [q_{d0}, q_{d1}, q_{d2}, q_{d3}]^T \in \mathbb{S}^3$ guaranteeing UAV stability and asymptotic convergence in a finite time. Tightly coupled cascaded control (to handle UAV underactuation) is proposed where the outer control, translational part (position and linear velocity control) is quaternion-based ABC while the inner control, rotational part (orientation and angular velocity control) is quaternion-based AFTSMC able to reduce

chattering, guarantee asymptotic stability, and ensure finite time convergence. The proposed controller utilizes four control inputs to control seven states $(q_0, q_1, q_2, q_3, x_p, y_p, z_p)$. The proposed control system is shown in Figure 2.

A. Adaptive Backstepping for Position Control

A quaternion-based ABC algorithm is designed for the UAV translation to track predefined desired translation trajectories to resolve persistent singularity issues in Euler-based controllers (e.g., [33]). Backstepping is a superior technique for underactuated systems because of its recursive approach for implementation [44]. The first step is to find the error between the UAV's true and desired position. Based on (6), the error equations $e_p = [e_{xp}, e_{yp}, e_{zp}]^T \in \mathbb{R}^3$ can be derived as follow:

$$\begin{aligned} e_{xp} &= x_p - x_d \\ e_{yp} &= y_p - y_d \\ e_{zp} &= z_p - z_d \end{aligned} \quad (9)$$

such that the derivative of (9) is given by

$$\begin{aligned} \dot{e}_{xp} &= \dot{x}_p - \dot{x}_d = v_1 - \dot{x}_d \\ \dot{e}_{yp} &= \dot{y}_p - \dot{y}_d = v_2 - \dot{y}_d \\ \dot{e}_{zp} &= \dot{z}_p - \dot{z}_d = v_3 - \dot{z}_d \end{aligned} \quad (10)$$

Let us define the following Lyapunov function candidate and subsequently formulate the controller that ensures system stability. Consider the following Lyapunov function:

$$\begin{aligned} V_1 &= \frac{1}{2}e_{xp}^2 \\ V_3 &= \frac{1}{2}e_{yp}^2 \\ V_5 &= \frac{1}{2}e_{zp}^2 \end{aligned} \quad (11)$$

In view of (11) and with the substitution of (10), one obtains

$$\begin{aligned} \dot{V}_1 &= e_{xp}(\dot{e}_{xp}) = e_{xp}(v_1 - \dot{x}_d) \\ \dot{V}_3 &= e_{yp}(\dot{e}_{yp}) = e_{yp}(v_2 - \dot{y}_d) \\ \dot{V}_5 &= e_{zp}(\dot{e}_{zp}) = e_{zp}(v_3 - \dot{z}_d) \end{aligned} \quad (12)$$

Therefore, v_{1d} , v_{2d} , and v_{3d} should be selected to stabilize (12) as follows:

$$\begin{aligned} v_{1d} &= -m_{xp}e_{xp} + \dot{x}_d \\ v_{2d} &= -m_{yp}e_{yp} + \dot{y}_d \\ v_{3d} &= -m_{zp}e_{zp} + \dot{z}_d \end{aligned} \quad (13)$$

where m_{xp} , m_{yp} , and m_{zp} are non-zero and non-negative constants. Consider the translation dynamics (6) and let Assumption 1 and 2 hold true. The position errors in (9) converges to origin if the desired v_{1d} , v_{2d} , and v_{3d} are selected as (13). It is obvious that e_{xp} , e_{yp} , and e_{zp} are converging to zero, if (12) becomes negative definite. One finds

$$\begin{aligned} \dot{V}_1 &= e_{xp}(\dot{e}_{xp}) = e_{xp}(-m_{xp}e_{xp} + \dot{x}_d - \dot{x}_d) \\ &= -m_{xp}e_{xp}^2 < 0 \\ \dot{V}_3 &= e_{yp}(\dot{e}_{yp}) = e_{yp}(-m_{yp}e_{yp} + \dot{y}_d - \dot{y}_d) \\ &= -m_{yp}e_{yp}^2 < 0 \\ \dot{V}_5 &= e_{zp}(\dot{e}_{zp}) = e_{zp}(-m_{zp}e_{zp} + \dot{z}_d - \dot{z}_d) \\ &= -m_{zp}e_{zp}^2 < 0 \end{aligned} \quad (14)$$

As a next step, we need to show that v_1 , v_2 , and v_3 are converging to v_{1d} , v_{2d} , and v_{3d} , respectively. Let us define the following set of errors:

$$\begin{aligned} e_{v1} &= v_1 - v_{1d} \\ e_{v2} &= v_2 - v_{2d} \\ e_{v3} &= v_3 - v_{3d} \end{aligned} \quad (15)$$

Similar to the previous step, consider selecting the following Lyapunov function candidate:

$$\begin{aligned} V_2 &= V_1 + \frac{1}{2}e_{v1}^2 \\ V_4 &= V_3 + \frac{1}{2}e_{v2}^2 \\ V_6 &= V_5 + \frac{1}{2}e_{v3}^2 \end{aligned} \quad (16)$$

In view of (14) and (16), one obtains

$$\begin{aligned} \dot{V}_2 &= \dot{V}_1 + e_{v1}\dot{e}_{v1} = -m_{xp}e_{xp}^2 + e_{v1}(\dot{v}_1 - \dot{v}_{1d}) \\ \dot{V}_4 &= \dot{V}_3 + e_{v2}\dot{e}_{v2} = -m_{yp}e_{yp}^2 + e_{v2}(\dot{v}_2 - \dot{v}_{2d}) \\ \dot{V}_6 &= \dot{V}_5 + e_{v3}\dot{e}_{v3} = -m_{zp}e_{zp}^2 + e_{v3}(\dot{v}_3 - \dot{v}_{3d}) \end{aligned} \quad (17)$$

where m_{xp} , m_{yp} , and m_{zp} are positive constants to be selected subsequently. One way to address the UAV underactuated issue is by utilizing the backstepping approach to generate intermediary control signals (virtual control). Now, U_x , U_y , and U_z are introduced as virtual controls (inner control) to generate the total thrust. Substituting (9), (10), and (13) in (16) and by using U_x , U_y , and U_z as virtual variables, the following equations are obtained as:

$$\begin{aligned} \dot{V}_2 &= -m_{xp}e_{xp}^2 + e_{v1}(U_x + (m_{xp}\dot{e}_{xp} - \ddot{x}_d)) \\ \dot{V}_4 &= -m_{yp}e_{yp}^2 + e_{v2}(U_y + (m_{yp}\dot{e}_{yp} - \ddot{y}_d)) \\ \dot{V}_6 &= -m_{zp}e_{zp}^2 + e_{v3}(U_z + (m_{zp}\dot{e}_{zp} - \ddot{z}_d)) \end{aligned} \quad (18)$$

By plugging \dot{e}_{xp} , \dot{e}_{yp} , and \dot{e}_{zp} from (10) and (13), the virtual control input U_x , U_y , U_z are designed as follows:

$$\begin{aligned} U_x &= m_{xp}^2 e_{xp} - \hat{n}_{x2} e_{v1} + \ddot{x}_d \\ U_y &= m_{yp}^2 e_{yp} - \hat{n}_{y2} e_{v2} + \ddot{y}_d \\ U_z &= m_{zp}^2 e_{zp} - \hat{n}_{z2} e_{v3} + \ddot{z}_d \end{aligned} \quad (19)$$

with \hat{n}_{x2} , \hat{n}_{y2} , and \hat{n}_{z2} being adaptive parameter estimation to automatically adjust position control parameters in terms of stability and the speed of convergence and their adaptation laws are given by:

$$\text{Update Law} \begin{cases} \dot{\hat{n}}_{x2} &= \eta_1 e_{v1}^2 \\ \dot{\hat{n}}_{y2} &= \eta_2 e_{v2}^2 \\ \dot{\hat{n}}_{z2} &= \eta_3 e_{v3}^2 \end{cases} \quad (20)$$

where η_1 , η_2 , and η_3 are positive constants.

Lemma 1. [33] *Based on Barbalet Lemma, if $f(s)$ is a uniformly bounded continuous function and $\lim_{s \rightarrow +\infty} \int_0^T f(s) ds$ exists, $f(s)$ converges to the origin asymptotically.*

Theorem 1. *The translation dynamics described in (6) are asymptotically stable if the UAV thrust is designed as follows:*

$$F_{th} = m\sqrt{U_x^2 + U_y^2 + (U_z + g)^2} \quad (21)$$

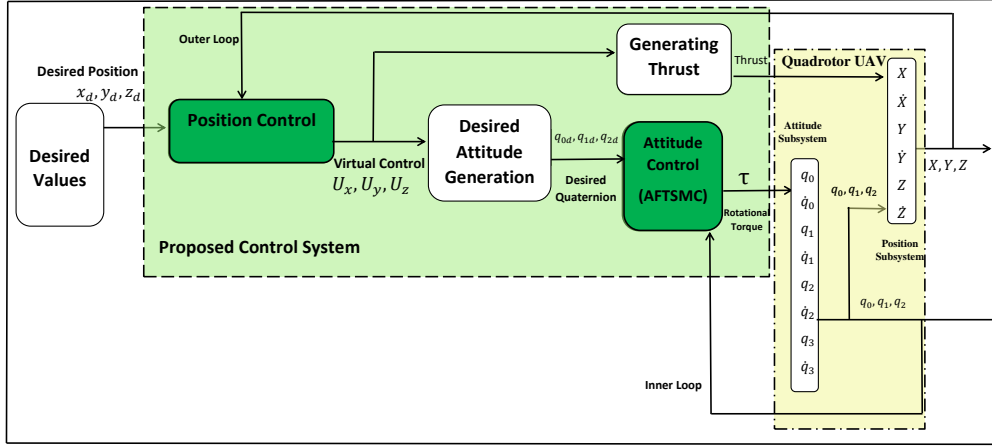


Fig. 2: Illustrative diagram of the proposed control system for UAV

where U_x , U_y , and U_z are calculated as in (19) with adaptation laws defined in (20).

Proof: To prove that the subsystem is stable and to determine \hat{n}_{x2} , \hat{n}_{y2} , and \hat{n}_{z2} , the Lyapunov candidate of position system is selected. Lemma 1 [33] is employed to ensure controller stability and error convergence. By substituting for the intermediary control laws in (19), the stability of the translation system is guaranteed as follows:

$$\begin{aligned} V_{tot} &= V_2 + V_4 + V_6 \\ &= \frac{1}{2}e_{xp}^2 + \frac{1}{2}e_{yp}^2 + \frac{1}{2}e_{zp}^2 + \frac{1}{2}e_{v1}^2 + \frac{1}{2}e_{v2}^2 + \frac{1}{2}e_{v3}^2 \\ &\quad + \frac{1}{2}\tilde{n}_{x2}^2 + \frac{1}{2}\tilde{n}_{y2}^2 + \frac{1}{2}\tilde{n}_{z2}^2 \end{aligned} \quad (22)$$

where $\tilde{n}_{x2} = \hat{n}_{x2} - n_{x2}$, $\tilde{n}_{y2} = \hat{n}_{y2} - n_{y2}$, and $\tilde{n}_{z2} = \hat{n}_{z2} - n_{z2}$. Based on (18), the derivative of (22) is computed as follows:

$$\dot{V}_{tot} = \dot{V}_2 + \dot{V}_4 + \dot{V}_6 + \tilde{n}_{x2}\dot{\tilde{n}}_{x2} + \tilde{n}_{y2}\dot{\tilde{n}}_{y2} + \tilde{n}_{z2}\dot{\tilde{n}}_{z2} \quad (23)$$

By inserting (19) in (18) and (23), the above equation is simplified as:

$$\begin{aligned} \dot{V}_{tot} &= -m_{xp}e_{xp}^2 - m_{yp}e_{yp}^2 - m_{zp}e_{zp}^2 - \hat{n}_{x2}e_{v1}^2 - \hat{n}_{y2}e_{v2}^2 \\ &\quad - \hat{n}_{z2}e_{v3}^2 + \tilde{n}_{x2}\dot{\tilde{n}}_{x2} + \tilde{n}_{y2}\dot{\tilde{n}}_{y2} + \tilde{n}_{z2}\dot{\tilde{n}}_{z2} \end{aligned} \quad (24)$$

Hence, by inserting (20) in the derivative of (24), the stability can be guaranteed such that:

$$\begin{aligned} \dot{V}_{tot} &= -m_{xp}e_{xp}^2 - m_{yp}e_{yp}^2 - m_{zp}e_{zp}^2 - (\tilde{n}_{x2} + n_{x2})e_{v1}^2 \\ &\quad - (\tilde{n}_{y2} + n_{y2})e_{v2}^2 - (\tilde{n}_{z2} + n_{z2})e_{v3}^2 + \tilde{n}_{x2}e_{v1}^2 + \tilde{n}_{y2}e_{v2}^2 \\ &\quad + \tilde{n}_{z2}e_{v3}^2 = -m_{xp}e_{xp}^2 - m_{yp}e_{yp}^2 - m_{zp}e_{yp}^2 - n_{x2}e_{v1}^2 \\ &\quad - n_{y2}e_{v2}^2 - n_{z2}e_{v3}^2 \leq 0 \end{aligned} \quad (25)$$

As (25) becomes negative definite for all $V_{tot} > 0$ and $\dot{V}_{tot} = 0$ only at $V_{tot} = 0$, it is ensured that the errors converge to the origin and the system is asymptotically stable.

Let us calculate the total thrust (F_{th}) necessary to control the UAV translation dynamics and generate the desired attitude

trajectories. Based on (6) and (19), the virtual controls U_x , U_y , and U_z can be re-expressed as :

$$\begin{aligned} U_x &= -2m^{-1}F_{th}(q_0q_2 + q_1q_3) \\ U_y &= -2m^{-1}F_{th}(q_2q_3 - q_0q_1) \\ U_z &= -m^{-1}F_{th}(q_0^2 - q_1^2 - q_2^2 + q_3^2) + g \end{aligned} \quad (26)$$

Solving for (26) one obtains the actual thrust F_{th} as follows:

$$F_{th} = m\sqrt{U_x^2 + U_y^2 + (U_z + g)^2} \quad (27)$$

Based on (27), it becomes obvious that the actual total thrust will not be subject to singularity at any time instant. In view of (26) and (21), the desired quaternion q_{0d} , q_{1d} , q_{2d} as follows:

$$\begin{aligned} q_{0d} &= \sqrt{\frac{m(g + U_z)}{2F_{th}} + \frac{1}{2}} \\ q_{1d} &= -\frac{mU_y}{2F_{th}q_{0d}} \\ q_{2d} &= \frac{mU_x}{2F_{th}q_{0d}} \end{aligned} \quad (28)$$

visit [11]. Note that it is assumed $q_{3d} = 0$. As a summary, in this section, quaternion-based ABC (outer control) is designed for the UAV translation dynamics with an objective of generating the total UAV thrust and desired quaternion components for attitude control. In the next section, a quaternion-based AFTSMC (inner control) will be developed for the UAV attitude control problem.

B. Fast Terminal Sliding Mode Control Attitude Control

In comparison with the conventional SMC, AFTSMC brings more advantages in terms of performance. AFTSMC significantly decreases chattering, which is a crucial factor for smooth trajectory tracking and actuator safety. Moreover, AFTSMC can address singularity issues of conventional SMC guaranteeing finite time convergence [45]. Consider the following attitude errors [42]:

$$\begin{aligned} e_0 &= q_0q_{0d} + \mathbf{q}_d\mathbf{q}^\top \\ e &= q_{0d}\mathbf{q} - q_0\mathbf{q}_d + [\mathbf{q}] \times \mathbf{q}_d \\ R_e &= RR_d^\top = (e_0^2 - e^\top e)\mathbf{I}_3 + 2ee^\top + 2e_0[e] \times \end{aligned} \quad (29)$$

where $e_0 \in \mathbb{R}$ and $e \in \mathbb{R}^3$ denoted quaternion error between UAV true and desired trajectories, $R \in SO(3)$ and R_d refers to true and desired rotation matrix of the UAV, respectively, and $R_e \in SO(3)$ denotes error in orientation. The goal is to drive $R \rightarrow R_d$ or in other words $R_e \rightarrow \mathbf{I}_3$. The equivalent unit-quaternion mapping is to drive $e_0 \rightarrow 1$ and $e \rightarrow 0_{3 \times 1}$. Let us define the error in angular velocity is defined by:

$$\Omega_e = \Omega_B - R_e \Omega_d \quad (30)$$

where the desired angular velocity Ω_d can be found using the following equation [42]:

$$\dot{Q}_d = (q_{0d} \mathbf{I}_3 + [q_d]_{\times}) \Omega_d \quad (31)$$

with $q_d = [q_{1d}, q_{2d}, q_{3d}]^T$. Based on (29), (30) and (5), the attitude error dynamic is obtained as [11]:

$$\text{Error dynamic} \begin{cases} \dot{e}_0 &= \frac{1}{2} e^T \Omega_e \\ \dot{e} &= \frac{1}{2} (e_0 \Omega_e + [e]_{\times} \Omega_e) \\ J \dot{\Omega}_e &= [J \Omega_B]_{\times} \Omega_B + \mathcal{T} + \\ &J [\Omega_e]_{\times} R_e \Omega_d - J R_e \dot{\Omega}_d \end{cases} \quad (32)$$

Let us move to the Quaternion-based AFTSMC and introduce the following sliding surface (32):

$$s = \dot{e} + \gamma_1 e + \gamma_2 e^{n/l} + \gamma_3 \Omega_e \quad (33)$$

where γ_1 and γ_2 are positive constants and $\gamma_3 = 1$. n and l are positive constants and $0 < \frac{n}{l} < 1$. The derivative of (33) is calculated as:

$$\dot{s} = \ddot{e} + \gamma_1 \dot{e} + \frac{n}{l} \gamma_2 e^{(n/l-1)} \dot{e} + \dot{\Omega}_e \quad (34)$$

Based on (34), it is obvious that when e becomes zero, $e^{(n/l-1)}$ could converge to infinity. In such case, the system could be subject to singularity and thereby become unstable. In view of [33], [46], to resolve this issue, the sliding surface described in (33) can be modified by switching threshold value to overcome the singularity issue as follows:

$$s = \dot{e} + \gamma_1 e + \gamma_2 \Delta(e) + \gamma_3 \Omega_e \quad (35)$$

where $\Delta(e)$ is defined as:

$$\Delta(e) = \begin{cases} e^{\frac{n}{l}}, & \text{if } s = 0 \text{ or } s \neq 0, |e| > \epsilon \\ e, & \text{if } s \neq 0, |e| \leq \epsilon \end{cases} \quad (36)$$

with ϵ being a small positive value. Based on (35) and (36), let us propose the attitude controller as follows:

$$\begin{aligned} \mathcal{T} = & - ([J \Omega_B]_{\times} \Omega_B + J [\Omega_e]_{\times} R_e \Omega_d - J R_e \dot{\Omega}_d) \\ & - \left(\frac{1}{2} e_0 + \frac{1}{2} [e]_{\times} \Omega_e + \mathcal{I} \right)^{-1} \left(\frac{1}{2} \dot{e}_0 \Omega_e + \frac{1}{2} [\dot{e}]_{\times} \Omega_e \right. \\ & \left. + \gamma_1 \dot{e} + \gamma_2 (n/l) e^{n/l-1} \dot{e} + \mu_1 s + \hat{\mathbf{K}} \text{sign}(s) \right) \end{aligned} \quad (37)$$

where μ_1 is a positive constant and the adaptive law for $\hat{\mathbf{K}} = [\hat{k}_1, \hat{k}_2, \hat{k}_3]^T$ is as follows:

$$\text{Update Law} \begin{cases} \dot{\hat{k}}_1 &= \lambda ||s|| \\ \dot{\hat{k}}_2 &= \lambda ||s|| \\ \dot{\hat{k}}_3 &= \lambda ||s|| \end{cases} \quad (38)$$

where $\lambda > 0$.

Theorem 2. *The attitude system (5) becomes asymptotically stable and the attitude error $Q_e = [e_0, e^T]^T \rightarrow [1, 0, 0, 0]^T$ and $\Omega_e \rightarrow 0$ when the proposed input controller is defined as (37) with the adaptation laws in (38).*

Proof: The Lyapunov approach and Lemma 1 are used to prove Theorem 2. Let us introduce the following Lyapunov function candidate:

$$V_s = \frac{1}{2} s^T s + \frac{1}{2\lambda} \tilde{\mathbf{K}}^T \tilde{\mathbf{K}} \quad (39)$$

where $\tilde{\mathbf{K}} = \hat{\mathbf{K}} - \mathbf{K}$. The derivative of (39) is obtained by:

$$\dot{V}_s = s \left(\ddot{e} + \gamma_1 \dot{e} + \gamma_2 \frac{n}{l} e^{n/l-1} \dot{e} + \dot{\Omega}_e \right) + \frac{1}{\lambda} \tilde{\mathbf{K}}^T \dot{\tilde{\mathbf{K}}} \quad (40)$$

Also, the \ddot{e} can be derived from (32) as:

$$\ddot{e} = \frac{1}{2} (\dot{e}_0 \Omega_e + e_0 \dot{\Omega}_e + [\dot{e}]_{\times} \Omega_e + [e]_{\times} \dot{\Omega}_e) \quad (41)$$

Using (1), (41) and (32), the above equation can be rewritten as follows:

$$\begin{aligned} \dot{V}_s = & s \left(\frac{1}{2} ((\dot{e}_0 \mathbf{I}_3 + [\dot{e}]_{\times}) \Omega_e + (e_0 \mathbf{I}_3 + [e]_{\times}) \dot{\Omega}_e) + \right. \\ & \left. \frac{\gamma_1}{2} (e_0 \Omega_e + [e]_{\times} \Omega_e) + \gamma_2 \frac{n}{l} e^{n/l-1} \dot{e} + J^{-1} ([J \Omega_B]_{\times} \Omega_B + \right. \\ & \left. \mathcal{T} + J [\Omega_e]_{\times} R_e \Omega_d - J R_e \dot{\Omega}_d) \right) + \frac{1}{\lambda} \tilde{\mathbf{K}}^T \dot{\tilde{\mathbf{K}}} \end{aligned} \quad (42)$$

By substituting (37) in (42), the derivative of (39) becomes:

$$\dot{V}_s = -\mu_1 ||s||^2 - s \hat{\mathbf{K}} \text{sign}(s) + \frac{1}{\lambda} \tilde{\mathbf{K}}^T \dot{\tilde{\mathbf{K}}} \quad (43)$$

Based on (38), the above equation can be rewritten as:

$$\begin{aligned} \dot{V}_s = & -\mu_1 ||s||^2 - s (\tilde{\mathbf{K}} + \mathbf{K}) \text{sign}(s) + \frac{1}{\lambda} \tilde{\mathbf{K}}^T \lambda ||s|| \\ \leq & -\mu_1 ||s||^2 - \mathbf{K} ||s|| \leq 0 \end{aligned} \quad (44)$$

Therefore, the attitude dynamics in (7) become asymptotically stable using the proposed controller in (37) completing the proof.

The proposed quaternion-based AFTSMC guarantees asymptotic convergence of the attitude dynamics. However, finite time convergence is not guaranteed. This issue will be addressed in the subsequent subsection.

C. Attitude Control and Finite Time Convergence

In this subsection, the finite time t_r of the AFTSMC is computed for the proposed controller (37). It is assumed that the time interval between the initial error values $[e(0) \neq 0, \Omega_e(0) \neq 0] \neq 0$ to reach $e = 0$ is t_r .

Lemma 2. *The state errors reach the AFTSMC surface in (35) using the controller (37) and adaptive update law (38) in a finite time t_r .*

Proof: To obtain finite time convergence, consider the following real value function:

$$V_{tr} = \frac{1}{2} s^2 \quad (45)$$

The derivative of (45) is obtained as:

$$\dot{V}_{tr} = s \left(\ddot{e} + \gamma_1 \dot{e} + \gamma_2 \frac{n}{l} e^{n/l-1} \dot{e} + \dot{\Omega}_e \right) \quad (46)$$

Using (37) and (1), the above expression (46) can be rewritten as follows:

$$\begin{aligned} \dot{V}_{tr} = & s\left(\frac{1}{2}((\dot{e}_0\mathbf{I}_3 + [\dot{e}]_{\times})\Omega_e + (e_0\mathbf{I}_3 + [e]_{\times})\dot{\Omega}_e) + \right. \\ & \left. \gamma_1\left(\frac{1}{2}(e_0\Omega_e + [e]_{\times}\Omega_e)\right) + \gamma_2\frac{n}{l}e^{n/l-1}\dot{e} + J^{-1}([J\Omega_B]_{\times}\Omega_B + \right. \\ & \left. \mathcal{T} + J[\Omega_e]_{\times}R_e\Omega_d - JR_e\dot{\Omega}_d)\right) \end{aligned} \quad (47)$$

Substituting for (37) in (47), one obtains:

$$\dot{V}_{tr} \leq -\frac{1}{2}\mu_1 s^2 - \mu_2 |s| \leq 0 \quad (48)$$

such that

$$\dot{V}_{tr} = \frac{dV_{tr}}{dt} \leq -\mu_1 V_{tr} - \mu_2 \sqrt{2}V_{tr}^{1/2} \quad (49)$$

Let us introduce the variable $\varrho = \mu_2 \sqrt{2}$. One finds:

$$dt \leq \frac{-dV_{tr}}{\mu_1 V_{tr} + \varrho V_{tr}^{1/2}} \quad (50)$$

such that

$$dt \leq \frac{-V_{tr}^{-1/2} dV_{tr}}{\mu_1 V_{tr}^{1/2} + \varrho} = -2 \frac{dV_{tr}^{1/2}}{\mu_1 V_{tr}^{1/2} + \varrho} \quad (51)$$

Integrating both sides of (51), the finite time can be derived as:

$$\begin{aligned} \int_0^{t_r} dt & \leq \int_{V_{tr}(0)}^{V_{tr}(t_r)} \frac{-2dV_{tr}^{1/2}}{\mu_1 V_{tr}^{1/2} + \varrho} \\ & = \left[\frac{-2}{\mu_1} \ln(\mu_1 V_{tr}^{1/2} + \varrho) \right]_{V_{tr}(0)}^{V_{tr}(t_r)} \end{aligned} \quad (52)$$

Finally, based on (52), t_r is calculated as:

$$t_r \leq \frac{2}{\mu_1} \ln\left(\frac{\mu_1 V_{tr}(0)^{1/2} + \varrho}{\varrho}\right) \quad (53)$$

According to (53), it is concluded that sliding surface s in (39) converges to zero, and states reach the desired values in finite time. Also, as long as $s = 0$, then error output and states converge to zero in finite time as well.

Finally, both pose and attitude quaternion-based are obtained in IV-A and IV-B sections, respectively. Stabilizing the UAV system and enhancing following the desired position and attitude trajectories are achieved by designing proposed controllers. The flight control diagram, which includes backstepping and AFTSMC, is shown in Figure 2. In the following section, the algorithm steps to design controllers are presented to facilitate controller implementation for the UAV.

V. IMPLEMENTATION STEPS

The implementation process of the proposed UAV controller is presented step by step in this section as follows:

Step 1. Define the initial values $X_0 = [x_p(0), y_p(0), z_p(0)]$, $Q_0 = [q_0(0), q_1(0), q_2(0), q_3(0)]^T$, and $\Omega_{B_0} = [p_v(0), q_v(0), r_v(0)]$. Calculate for R and R_d as follows:

$$\begin{aligned} R & = (q_0^2 - \mathbf{q}^T \mathbf{q}) I_3 + 2\mathbf{q}\mathbf{q}^T + 2q_0[\mathbf{q}]_{\times} \\ R_d & = (q_{d0}^2 - \mathbf{q}_d^T \mathbf{q}_d) I_3 + 2\mathbf{q}_d \mathbf{q}_d^T + 2q_{d0}[\mathbf{q}_d]_{\times} \end{aligned} \quad (54)$$

Step 2. Set UAV's desired position trajectory: $X_d = [x_d, y_d, z_d]^T$

Step 3. Calculate position errors using (9):

$$\begin{aligned} e_{xp} & = x_p - x_d \\ e_{yp} & = y_p - y_d \\ e_{zp} & = z_p - z_d \end{aligned}$$

and follow (13), (14) to design virtual v_{1d} , v_{2d} , and v_{3d} :

$$\begin{aligned} v_{1d} & = -m_{xp}e_{xp} + \dot{x}_d \\ v_{2d} & = -m_{yp}e_{yp} + \dot{y}_d \\ v_{3d} & = -m_{zp}e_{zp} + \dot{z}_d \end{aligned}$$

and find:

$$\begin{aligned} e_{v1} & = v_1 - v_{1d} \\ e_{v2} & = v_2 - v_{2d} \\ e_{v3} & = v_3 - v_{3d} \end{aligned}$$

Step 4. Design and implement the ABC control for translation dynamics with the update laws in (19) and (20):

$$\begin{aligned} U_x & = -m_{xp}^2 e_{xp} - \hat{n}_{x2} e_{v1} + \ddot{x}_d \\ U_y & = -m_{yp}^2 e_{yp} - \hat{n}_{y2} e_{v2} + \ddot{y}_d \\ U_z & = -m_{zp}^2 e_{zp} - \hat{n}_{z2} e_{v3} + \ddot{z}_d \end{aligned}$$

where the control parameter adaptation to compensate for uncertainties are given by:

$$\text{Adaptive update} \begin{cases} \dot{\hat{n}}_{x2} & = \eta_1 e_{v1}^2 \\ \dot{\hat{n}}_{y2} & = \eta_2 e_{v2}^2 \\ \dot{\hat{n}}_{z2} & = \eta_3 e_{v3}^2 \end{cases}$$

Step 5. Find the actual thrust using the previous step as follows:

$$F_{th} = m\sqrt{U_x^2 + U_y^2 + (U_z + g)^2}$$

Step 6. Generate the desired attitude and angular velocity using (30) and (34) as follows:

$$\begin{aligned} q_{0d} & = \sqrt{\frac{m(g + U_z)}{2F_{th}} + \frac{1}{2}} \\ q_{1d} & = -\frac{mU_y}{2F_{th}q_{0d}} \\ q_{2d} & = \frac{mU_x}{2F_{th}q_{0d}} \\ q_{3d} & = 0 \end{aligned}$$

Step 7. Calculate attitude errors using (31) to (33):

$$\begin{aligned} e_0 & = q_0 q_{0d} + \mathbf{q}_d \mathbf{q}^T \\ e & = q_{0d} \mathbf{q} - q_0 \mathbf{q}_d + [\mathbf{q}]_{\times} \mathbf{Q}_d \\ R_e & = RR_d^T \end{aligned}$$

Step 8. Build the AFTSMC sliding surface using (40) and (41) as:

$$s = \dot{e} + \gamma_1 e + \gamma_2 \Delta(e) + \gamma_3 \Omega_e$$

Step 9. Implement AFTSMC attitude controller using (41)

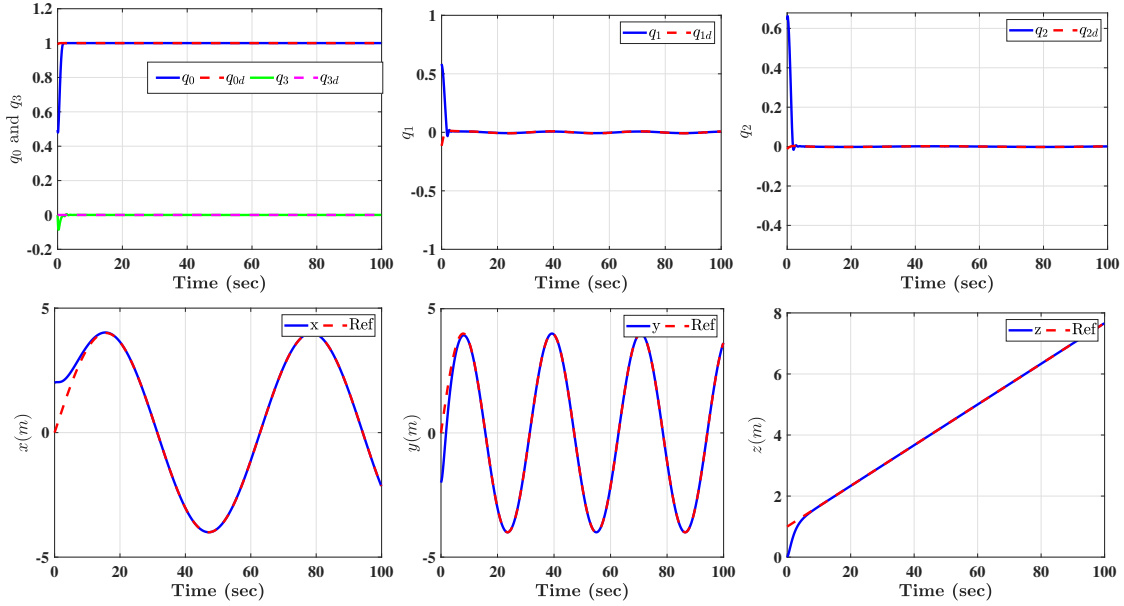


Fig. 3: UAV Attitude and Position Trajectory Tracking: True value represented in the blue solid-line, while red dash-lines plotted references

and the attitude adaptive law (38).

$$\begin{aligned} \mathcal{T} = & -([J\Omega_B]_{\times}\Omega_B + J[\Omega_e]_{\times}R_e\Omega_d - JR_e\dot{\Omega}_d) \\ & - \left(\frac{1}{2}e_0 + \frac{1}{2}[e]_{\times}\Omega_e + \mathcal{I}\right)^{-1} \left(\frac{1}{2}\dot{e}_0\Omega_e + \frac{1}{2}[\dot{e}]_{\times}\Omega_e \right. \\ & \left. + \gamma_1\dot{e} + \gamma_2(n/l)e^{n/l-1}\dot{e} + \mu_1s + \hat{K}sign(s)\right) \end{aligned}$$

with Adaptive update to minimize chattering:

$$\text{Adaptive update} \begin{cases} \dot{\hat{k}}_1 = \lambda||s|| \\ \dot{\hat{k}}_2 = \lambda||s|| \\ \dot{\hat{k}}_3 = \lambda||s|| \end{cases}$$

Step 10. Once the rotational torque ($\mathcal{T} = [\tau_1, \tau_2, \tau_3]^T$) and thrust (F_{th}) are obtained, the required drone rotor speeds are calculated by [12]:

$$\begin{bmatrix} \omega_1^2 \\ \omega_2^2 \\ \omega_3^2 \\ \omega_4^2 \end{bmatrix} = \begin{bmatrix} c_d & -c_d & c_d & -c_d \\ -l_d b_d & 0 & l_d b_d & 0 \\ 0 & -l_d b_d & 0 & l_d b_d \\ b_d & b_d & b_d & b_d \end{bmatrix}^{-1} \begin{bmatrix} \tau_1 \\ \tau_2 \\ \tau_3 \\ F_{th} \end{bmatrix}$$

where c_d refers to drag coefficient, l_d denotes the distance between the quadrotor center of mass, b_d refers to thrust factor, and $\omega_1, \omega_2, \omega_3$, and ω_4 refer to rotors speed.

Step 11. To address the chattering problem, one can replace $sign(\cdot)$ function (discontinuous part) with the $\tanh(\cdot)$ function. Repeat Steps 3 to 10.

VI. SIMULATION RESULTS

In this section, the simulation is conducted to demonstrate the effectiveness and robustness of the proposed quaternion-based controllers. We study the proposed quaternion-based ABC and AFTSMC performance for the translational and rotational dynamic of the underactuated quadrotor UAV. Firstly,

the proposed control system is performed to verify its performance in handling unknown time-varying uncertainties. Subsequently, we present comparative simulation outcomes to demonstrate the superiority, stability, and singularity-free of the developed quaternion-based controllers compared to the Euler-based established method in the literature. Table. II provides physical system and control design parameters.

A. Simulation Scenario

In this section, the simulation is conducted to verify the robustness of the proposed quaternion-based controllers by applying unknown time-varying uncertainties of parameters such as $0.025\sin(0.03t + 0.3)$, $0.03\sin(0.02t + 0.25)$, $0.04\sin(0.04t + 0.35)$, and $0.035\sin(0.015t + 0.4)$. We study the proposed quaternion-based ABC and AFTSMC performance for the translational and rotational dynamic of the underactuated quadrotor UAV. Firstly, the proposed control system is performed to verify its performance in handling unknown time-varying uncertainties. Subsequently, we present comparative simulation outcomes to demonstrate the superiority, stability, and singularity-free of the developed quaternion-based controllers compared to the Euler-based established method in the literature.

The performance of the proposed controllers is shown in Figure 3-6. In Figure 3, the attitude and position trajectories follow desired values; meanwhile, attitude desired values are generated by total thrust to address underactuated complexity of the UAV. Figure 4 presents the attitude control \mathcal{T} and total thrust F_{th} , respectively. According to Figure 4, the controller is robust and smooth. Also, the quaternion-based AFTSMC is robust to uncertainties without singularity and chattering issues. Figure 5 shows adaptive control parameters from (38) and (20). Figure 5 presents bounded adaptive estimates. The

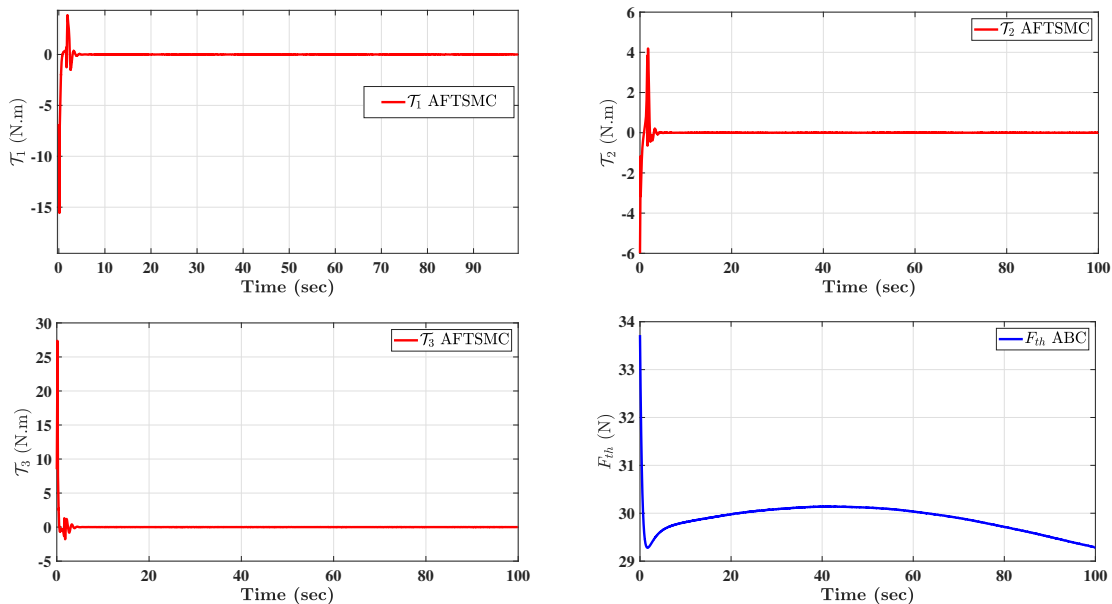


Fig. 4: UAV Rotational Control (plotted in red) and Total Thrust Input (represented in blue).

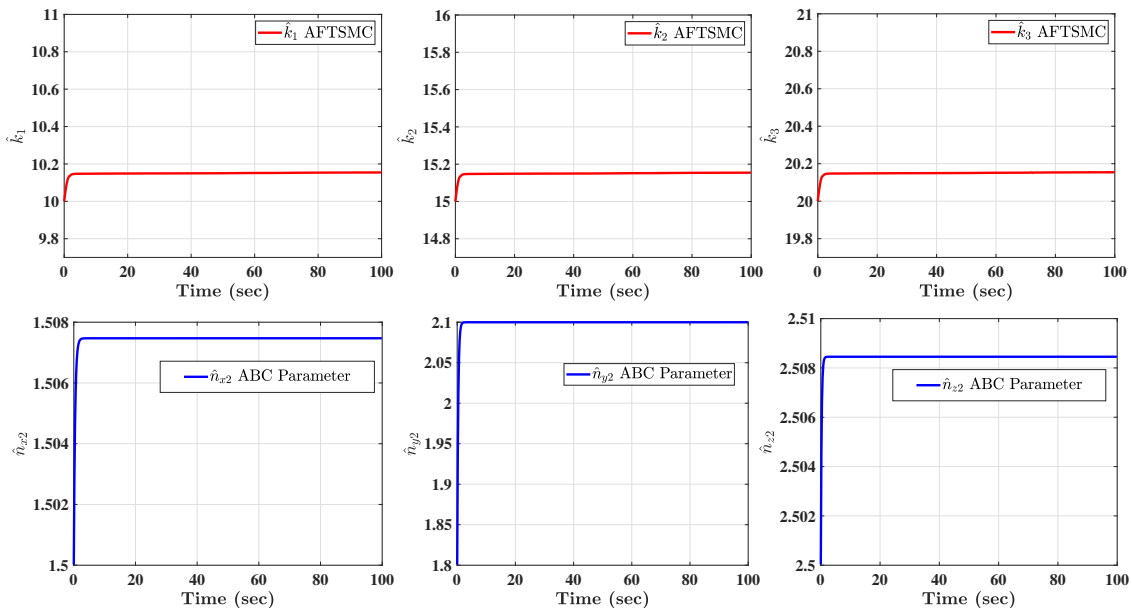


Fig. 5: Bounded and smooth trajectory of the adaptive parameters of controllers.

quaternion error, position error, angular velocity error, linear velocity error, and flight trajectory of UAV are shown in Figure 6. The error components converge successfully and smoothly to the origin.

The simulation results demonstrated in this paper validate the effectiveness of the proposed controllers, particularly in handling unknown time-varying uncertainties. The UAV performed excellent tracking capabilities and stability during the mission, as depicted in Figure 3. Theorem 1 and Lemma 1 guarantee the asymptotic stability of the UAV's translation dynamics, which confirms the simulation results shown in Figure

3. The figure depicts that the UAV's position is stable and smoothly tracks the desired trajectories with strong accuracy while significant initialization is applied. Moreover, Theorem 2 validates the convergence of the UAV's attitude states, as also shown by Figure 3. The quaternion orientations effectively follow the desired values generated by the thrust to address the underactuated complexity, and the attitude tracking under control law in equation (38) achieves asymptotic stability.

Results in Figure 4 depict that the proposed quaternion-based AFTSMC is highly effective in mitigating chattering issues, and its performance is outstanding in bringing states

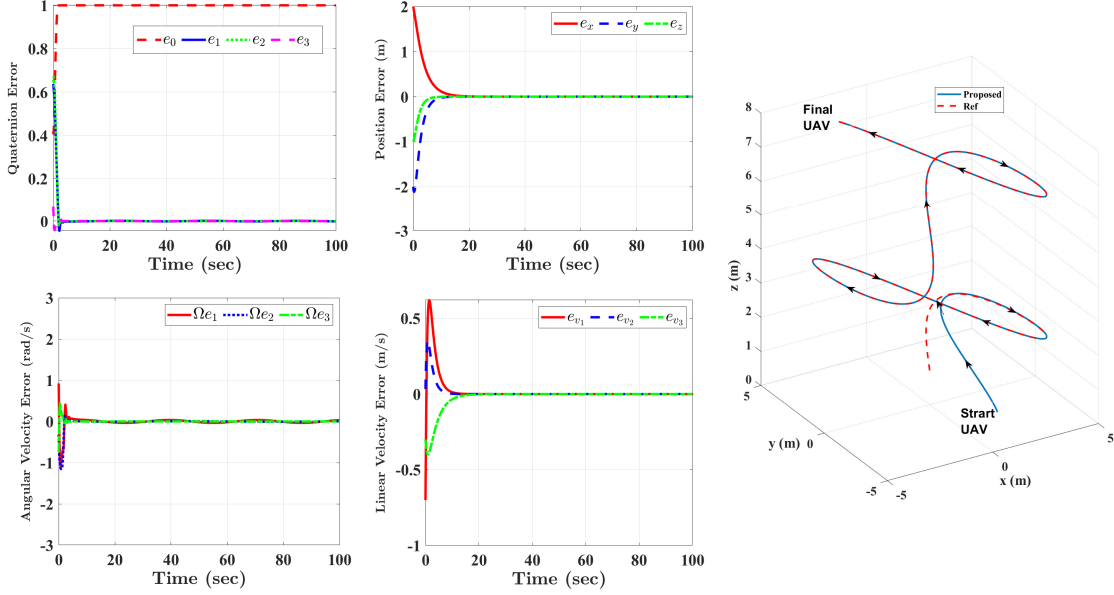


Fig. 6: UAV flight trajectories and Errors of the proposed quaternion-based AFTSMC.

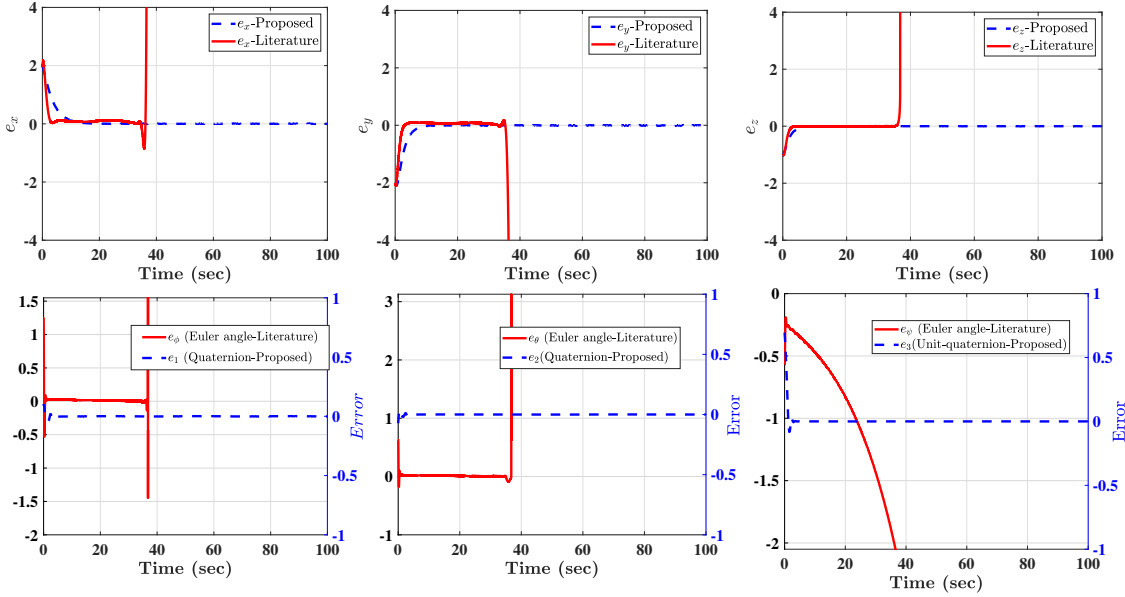


Fig. 7: Position and attitude error comparison between literature [33] and proposed work: Euler angles-based from literature [33] plotted in red solid line vs the proposed quaternion-based ABC with AFTSMC approach plotted in blue dash-line.

TABLE II: Physical system and control design parameters.

Parameters	Value	Parameters	Value
m_{xp}	0.3	m	3kg
m_{yp}	0.5	I_{xx}	$1.5kg.m^2$
m_{zp}	0.6	I_{yy}	$1.5kg.m^2$
γ_1	10	I_{zz}	$3kg.m^2$
γ_2	30	g	$9.8m/s^2$
γ_3	1	x_d	$4\cos(0.1t)$
$\eta_1 = \eta_2 = \eta_3$	0.01	y_d	$4\cos(0.2t)$
n	3	z_d	$(1/15)t + 1$
l	5	λ	30

to the desired values in finite time. Additionally, the total thrust successfully adjusts and adapts its performance to produce accurate and sufficient desired attitude orientations for rotational control, while the underactuated UAV works under parameter uncertainties. To handle the uncertainties, the adaptive features of the proposed controller update control parameters as shown in Figure 5. It confirms that the updated control parameters remain bounded and realistic. Also, \hat{K} in (37) is to reduce chattering in the attitude controller, while \hat{n}_{x2} , \hat{n}_{y2} , and \hat{n}_{z2} have a critical role in the speed of convergence and stability. The 6 DOF UAV flight trajectory exhibits not only smoothness but also accuracy. As illustrated in Figure

6, the developed controllers successfully achieve the defined goals, including trajectory tracking and minimizing chattering issues. Notably, the position and linear velocity errors converge to zero regardless of significant initial conditions. Additionally, the Unit-quaternion orientations converge the desired values of $[1, 0, 0, 0]$; meanwhile, angular velocity errors attain zero. The outstanding outcomes confirm the efficacy of the sliding surface defined in (35), as it brings the system states to the desired values in finite time.

B. Comparison

A comprehensive comparison is performed to demonstrate the state-of-the-art proposed quaternion-based controllers' performance over the Euler angle-based counterparts (e.g., [33]). The main shortcoming of Euler angle-based controllers stems from kinematic and model representation singularities, which often result in issues such as system instability and control failure. To highlight the differences, Figure 7 depicts the assessment of the attitude and position errors of both approaches. The results provide valuable insights into the advantages of using the proposed quaternion-based controller in UAV flight control, validating robustness and effectiveness in overcoming the deficiencies associated with Euler angle-based approaches.

Results demonstrate the success of the proposed quaternion-based controllers in accurately tracking attitude and position trajectories. In contrast, the Euler angle-based controllers exhibit limitations, failing to capture orientation in certain configurations. The validation further establishes that employing the Euler angle-based control system may lead to instability, and in some cases, it becomes kinematic singular, as depicted in Figure 7. Conversely, the innovative quaternion-based control system effectively addresses singularities, providing a robust and globally singularity-free model for quadrotors. Indeed, the validated superiority performance of the quaternion-based approach emphasizes its remarkable ability to address the limitations of Euler angle-based methods for controlling UAV flight. The successful mitigation of singularities and improved model representation make the proposed quaternion-based control system a viable solution for enhancing UAV performance and safety during flight missions.

VII. CONCLUSION

This paper proposed a novel quaternion-based attitude and position control for the underactuated UAV. The newly proposed quaternion-based Adaptive Backstepping Control (ABC) addressed the complexity of controlling the underactuated Unmanned Aerial Vehicle (UAV) system. The developed quaternion-based Adaptive Fast Terminal Sliding Mode Control (AFTSMC) was conducted to mitigate the chattering issue and guarantee finite time convergence of orientations and angular velocity. Precise tracking and asymptotic stability of translational and rotational dynamics were guaranteed by utilizing the Lyapunov theorem and Barbalet Lemma. The novel adaptive feature of controllers successfully handled the persistent unknown-time varying parameter uncertainties by adjusting control parameters. In fact, designing controllers based on unit-quaternion addressed the kinematic and model

singularity of other established approaches (e.g., Euler angles). Simulation results validated the efficacy of the proposed quaternion-based controllers in terms of stability, singularity, and chattering issues. Moreover, the results showed the outstanding performance of ABC and AFTSMC in accurate tracking in the presence of parameter uncertainties.

VIII. DISCLOSURE STATEMENT

No potential conflict of interest was reported by the author(s).

IX. DATA AVAILABILITY STATEMENT

The authors confirm that the data supporting the findings of this study are available within the article and its supplementary materials. The codes are available from the corresponding author upon reasonable request.

REFERENCES

- [1] H. A. Hashim, "A geometric nonlinear stochastic filter for simultaneous localization and mapping," *Aerospace Science and Technology*, vol. 111, p. 106569, 2021.
- [2] Y. F. Chen, N. K. Ure, G. Chowdhary, J. P. How, and J. Vian, "Planning for large-scale multiagent problems via hierarchical decomposition with applications to UAV health management," in *2014 American Control Conference*. IEEE, 2014, pp. 1279–1285.
- [3] N. Cheng, S. Wu, X. Wang, Z. Yin, C. Li, W. Chen, and F. Chen, "Ai for UAV-assisted iot applications: A comprehensive review," *IEEE Internet of Things Journal*, 2023.
- [4] H. A. Hashim, A. E. Eltoukhy, and K. G. Vamvoudakis, "UWB ranging and IMU data fusion: Overview and nonlinear stochastic filter for inertial navigation," *IEEE Transactions on Intelligent Transportation Systems*, 2023.
- [5] A. Khan, E. Yanmaz, and B. Rinner, "Information exchange and decision making in micro aerial vehicle networks for cooperative search," *IEEE Transactions on Control of Network Systems*, vol. 2, no. 4, pp. 335–347, 2015.
- [6] R. Bardera, A. A. Rodriguez-Sevillano, E. Barroso, and J. C. Matias, "Numerical analysis of a biomimetic UAV with variable length grids wingtips," *Results in Engineering*, vol. 18, p. 101087, 2023.
- [7] Y. Huo, X. Dong, T. Lu, W. Xu, and M. Yuen, "Distributed and multilayer UAV networks for next-generation wireless communication and power transfer: A feasibility study," *IEEE Internet of Things Journal*, vol. 6, no. 4, pp. 7103–7115, 2019.
- [8] L. Bartolomei, L. Teixeira, and M. Chli, "Fast multi-UAV decentralized exploration of forests," *IEEE Robotics and Automation Letters*, 2023.
- [9] A. V. Jonnalagadda and H. A. Hashim, "SegNet: A segmented deep learning based convolutional neural network approach for drones wildfire detection," *Remote Sensing Applications: Society and Environment*, p. 101181, 2024.
- [10] M. Hassanalian and A. Abdelkefi, "Classifications, applications, and design challenges of drones: A review," *Progress in Aerospace Sciences*, vol. 91, pp. 99–131, 2017.
- [11] H. A. Hashim, A. E. Eltoukhy, and A. Odry, "Observer-based controller for vtol-UAVs tracking using direct vision-aided inertial navigation measurements," *ISA transactions*, vol. 137, pp. 133–143, 2023.
- [12] H. A. Hashim, "Exponentially stable observer-based controller for VTOL-UAVs without velocity measurements," *International Journal of Control*, vol. 96, no. 8, pp. 1946–1960, 2023.
- [13] D. Wanner, H. A. Hashim, S. Srivastava, and A. Steinhauer, "Uav avionics safety, certification, accidents, redundancy, integrity, and reliability: a comprehensive review and future trends," *Drone Systems and Applications*, vol. 12, pp. 1–23, 2024.
- [14] Y. Du, P. Huang, Y. Cheng, Y. Fan, and Y. Yuan, "Fault tolerant control of a quadrotor unmanned aerial vehicle based on active disturbance rejection control and two-stage kalman filter," *IEEE Access*, 2023.
- [15] C. Wang, B. Song, P. Huang, and C. Tang, "Trajectory tracking control for quadrotor robot subject to payload variation and wind gust disturbance," *Journal of Intelligent & Robotic Systems*, vol. 83, pp. 315–333, 2016.

- [16] H. Liu, J. Xi, and Y. Zhong, "Robust attitude stabilization for nonlinear quadrotor systems with uncertainties and delays," *IEEE Transactions on Industrial Electronics*, vol. 64, no. 7, pp. 5585–5594, 2017.
- [17] T. Ryan and H. J. Kim, "Lmi-based gain synthesis for simple robust quadrotor control," *IEEE Transactions on Automation Science and Engineering*, vol. 10, no. 4, pp. 1173–1178, 2013.
- [18] I. Lopez-Sanchez and J. Moreno-Valenzuela, "Pid control of quadrotor UAVs: A survey," *Annual Reviews in Control*, vol. 56, p. 100900, 2023.
- [19] L. Martins, C. Cardeira, and P. Oliveira, "Linear quadratic regulator for trajectory tracking of a quadrotor," *IFAC-PapersOnLine*, vol. 52, no. 12, pp. 176–181, 2019.
- [20] O. Mofid, S. Mobayen, C. Zhang, and B. Esakki, "Desired tracking of delayed quadrotor UAV under model uncertainty and wind disturbance using adaptive super-twisting terminal sliding mode control," *ISA transactions*, vol. 123, pp. 455–471, 2022.
- [21] B. Lindqvist, S. S. Mansouri, A.-a. Agha-mohammadi, and G. Nikolakopoulos, "Nonlinear mpc for collision avoidance and control of UAVs with dynamic obstacles," *IEEE robotics and automation letters*, vol. 5, no. 4, pp. 6001–6008, 2020.
- [22] J. Willis, J. Johnson, and R. W. Beard, "State-dependent lqr control for a tilt-rotor UAV," in *2020 American Control Conference (ACC)*. IEEE, 2020, pp. 4175–4181.
- [23] D. Sacconi, L. Cecchin, and L. Fagiano, "Multitrajectory model predictive control for safe UAV navigation in an unknown environment," *IEEE Transactions on Control Systems Technology*, 2022.
- [24] K. Zhang, Y. Shi, and H. Sheng, "Robust nonlinear model predictive control based visual servoing of quadrotor UAVs," *IEEE/ASME Transactions on Mechatronics*, vol. 26, no. 2, pp. 700–708, 2021.
- [25] A. M. Ali, H. A. Hashim, and C. Shen, "MPC based linear equivalence with control barrier functions for VTOL-UAVs," in *2024 IEEE American Control Conference (ACC)*, 2024, pp. 1–6.
- [26] M. Vahdanipour and M. Khodabandeh, "Adaptive fractional order sliding mode control for a quadrotor with a varying load," *Aerospace Science and Technology*, vol. 86, pp. 737–747, 2019.
- [27] J. Baek, M. Jin, and S. Han, "A new adaptive sliding-mode control scheme for application to robot manipulators," *IEEE Transactions on industrial electronics*, vol. 63, no. 6, pp. 3628–3637, 2016.
- [28] M. T. Islam, K. Yoshida, S. Nishiyama, and K. Sakai, "Mutual validation of remote hydraulic estimates and flow model simulations using UAV-borne lidar and deep learning-based imaging techniques," *Results in Engineering*, vol. 20, p. 101415, 2023.
- [29] L. Medina, G. Guerra, M. Herrera, L. Guevara, and O. Camacho, "Trajectory tracking for non-holonomic mobile robots: A comparison of sliding mode control approaches," *Results in Engineering*, p. 102105, 2024.
- [30] S. Mobayen, "Design of cnf-based nonlinear integral sliding surface for matched uncertain linear systems with multiple state-delays," *Nonlinear Dynamics*, vol. 77, no. 3, pp. 1047–1054, 2014.
- [31] R. Alicka, E. M. Mellouli, and E. H. Tissir, "A modified sliding mode controller based on fuzzy logic to control the longitudinal dynamics of the autonomous vehicle," *Results in Engineering*, p. 102120, 2024.
- [32] M. said Adouairi, B. Bossoufi, S. Motahhir, and I. Saady, "Application of fuzzy sliding mode control on a single-stage grid-connected pv system based on the voltage-oriented control strategy," *Results in Engineering*, vol. 17, p. 100822, 2023.
- [33] M. Labbadi and M. Cherkaoui, "Robust adaptive backstepping fast terminal sliding mode controller for uncertain quadrotor UAV," *Aerospace Science and Technology*, vol. 93, p. 105306, 2019.
- [34] M. Labbadi, Y. Boukal, and M. Cherkaoui, "Path following control of quadrotor UAV with continuous fractional-order super twisting sliding mode," *Journal of Intelligent & Robotic Systems*, vol. 100, pp. 1429–1451, 2020.
- [35] O. Mofid and S. Mobayen, "Adaptive finite-time backstepping global sliding mode tracker of quad-rotor UAVs under model uncertainty, wind perturbation, and input saturation," *IEEE Transactions on Aerospace and Electronic Systems*, vol. 58, no. 1, pp. 140–151, 2021.
- [36] F. Zheng, T. Fan, M. Xu, J. Zhang, and F. Cheng, "Adaptive fractional order non-singular terminal sliding mode anti-disturbance control for advanced layout carrier-based UAV," *Aerospace Science and Technology*, vol. 139, p. 108367, 2023.
- [37] J. Sanwale, S. Dahiya, P. Trivedi, and M. Kothari, "Robust fault-tolerant adaptive integral dynamic sliding mode control using finite-time disturbance observer for coaxial octorotor UAVs," *Control Engineering Practice*, vol. 135, p. 105495, 2023.
- [38] K. Ahmadi, D. Asadi, A. Merheb, S.-Y. Nabavi-Chashmi, and O. Tutsoy, "Active fault-tolerant control of quadrotor UAVs with nonlinear observer-based sliding mode control validated through hardware in the loop experiments," *Control Engineering Practice*, vol. 137, p. 105557, 2023.
- [39] B. Gao, Y.-J. Liu, and L. Liu, "Adaptive neural fault-tolerant control of a quadrotor UAV via fast terminal sliding mode," *Aerospace Science and Technology*, p. 107818, 2022.
- [40] T. Xie, B. Xian, and X. Gu, "Fixed-time convergence attitude control for a tilt trirotor unmanned aerial vehicle based on reinforcement learning," *ISA transactions*, vol. 132, pp. 477–489, 2023.
- [41] C. Kwan and F. L. Lewis, "Robust backstepping control of nonlinear systems using neural networks," *IEEE Transactions on Systems, Man, and Cybernetics-Part A: Systems and Humans*, vol. 30, no. 6, pp. 753–766, 2000.
- [42] H. A. Hashim, "Special Orthogonal Group SO(3), Euler Angles, Angle-axis, Rodriguez Vector and Unit-quaternion: Overview, Mapping and Challenges," *ArXiv preprint ArXiv:1909.06669*, 2019.
- [43] J. Espin, C. Camacho, and O. Camacho, "Control of non-self-regulating processes with long time delays using hybrid sliding mode control approaches," *Results in Engineering*, vol. 22, p. 102113, 2024.
- [44] Y. Zhao, X. Sun, G. Wang, and Y. Fan, "Adaptive backstepping sliding mode tracking control for underactuated unmanned surface vehicle with disturbances and input saturation," *Ieee Access*, vol. 9, pp. 1304–1312, 2020.
- [45] S. Mobayen, "An adaptive fast terminal sliding mode control combined with global sliding mode scheme for tracking control of uncertain nonlinear third-order systems," *Nonlinear Dynamics*, vol. 82, no. 1-2, pp. 599–610, 2015.
- [46] C. Hua, J. Chen, and X. Guan, "Fractional-order sliding mode control of uncertain QUAVs with time-varying state constraints," *Nonlinear Dynamics*, vol. 95, pp. 1347–1360, 2019.